Electronic Supplementary Material (ESI) for Journal of Materials Chemistry C.
This journal is © The Royal Society of Chemistry 2016

A novel $p-$type half-Heusler from high-throughput transport and defect calculations

Sandip Bhattacharya
CMAT, ICAMS, Ruhr-Universität Bochum, 44780 Bochum, Germany

Georg K. H. Madsen
Institute of Materials Chemistry, TU Wien , A-1060 Vienna, Austria
(Dated: November 11, 2016)

PACS numbers:

Defect energetics for all seven HHCs

Here we list the detailed results for the defect formation energies (both intrinsic and extrinsic) defects of all seven HHCs investigated in the main paper. In the following, for the sake of clear illustration of the defect formation energies, unstable defects will not be shown.

The defect calculations were performed on a $4 \times 4 \times 4$ super-cell (196 atoms) with $4 \times 4 \times 4$ k-mesh using the VASP code.[5]. The super-cell size has also been tested by us previously for TiNiSn and TiCoSb HHCs[6].

Energy correction to defect formation energy

The formation energy of a particular defect is evaluated from Eq. (2) (Main paper), using the super-cell approach. However, when estimating the energies of the charged defect $E_{D^{(q)}}$ in Eq. (2), one needs the following corrections to the DFT energies,

$$\Delta E_{\rm corr} = \Delta E_{\rm VBM} + \Delta E_{\rm MP}(q) + \Delta E_{\rm PA}[D^{(q)}]. \tag{1}$$

The electronic chemical potential, μ_e, is always measured with respect to the VBM of the pristine super-cell. In the charged defect, $\Delta E_{\rm VBM}$ aligns the top of the valence band of the defected and non-defected cell. To remove the spurios effect of interaction between image charges in a finite super-cell, multipole corrections are implemented according to the method of Makov and Payne[1]. The correction $\Delta E_{\rm MP}(q)$ is given by,

$$\Delta E_{\rm MP}(q) = \frac{q^2 M}{2L\epsilon} + \mathcal{O}(L^{-3}), \tag{2}$$

here M is the Madelung constant of the supercell Bravais lattice, ϵ is the static di-electric constant, L is the distance between defect centers. ϵ is obtained from VASP using Density Functional Perturbation Theory.[2].

The net charge of the super-cell is compensated by a constant background charge. In this case, the Kohn-Sham eigenvalues are only defined up to a constant, which in-turn depends on the average crystal potential. This potential in the defect containing super-cell and in bulk must be aligned[3,4]. The total energies of the super-cells containing charged defects and the pristine bulk are corrected by, $\Delta E_{\rm PA}[D^{(q)}] = q[V_R(D^{(q)}) - V_R^{\rm bulk}]$. Here the term $V_R(D^{(q)}) - V_R^{\rm bulk}$ is the difference between the potentials at a reference point R, for the charged defect and the pristine (bulk) super-cell. Thus the creation of a defect results in a constant shift in the potential V_R.

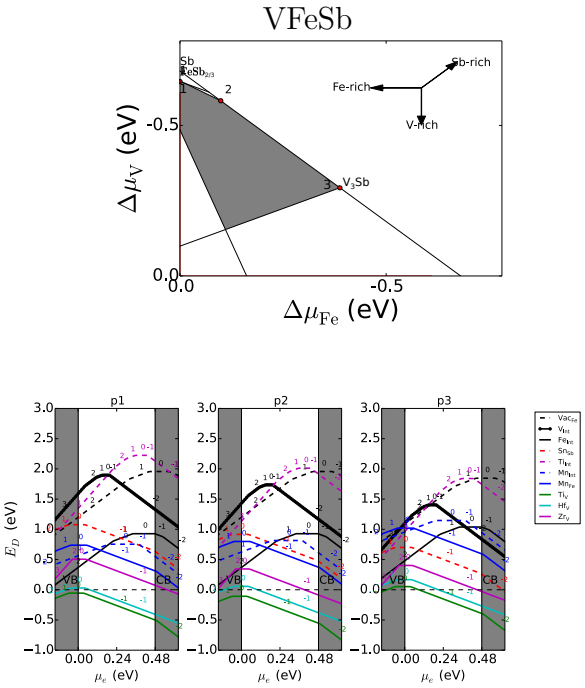

FIG. 1: The atomic chemical potential ($\Delta\mu_\alpha$, α is V, Fe and Sb) stability window that would eliminate the formation of competing phases and result in thermodynamically stable VCoSn is shown in grey (top). The energy of formation of most stable intrinsic defects (anti-sites, interstitials, vacancies) and extrinsic defects as a function of electronic chemical potential, μ_e. The energies are evaluated at three points in the boundaries of the $\Delta\mu_\alpha$ window.

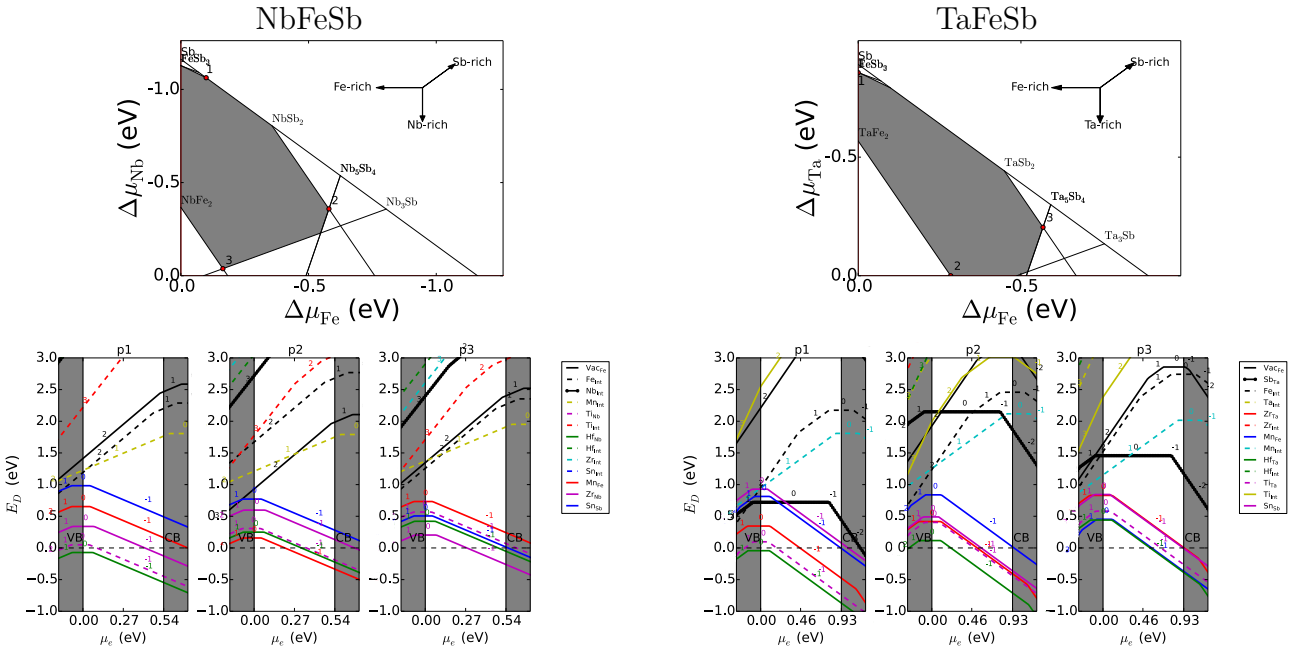

FIG. 2: The atomic chemical potential ($\Delta\mu_\alpha$, α is Nb/Ta, Fe and Sb) stability window that would eliminate the formation of competing phases and result in thermodynamically stable NbCoSn (left) and TaCoSn (right) are shown in grey (top). The energy of formation of most stable intrinsic defects (anti-sites, interstitials, vacancies) and extrinsic defects as a function of electronic chemical potential, μ_e. The energies are evaluated at three points in the boundaries of the $\Delta\mu_\alpha$ window.

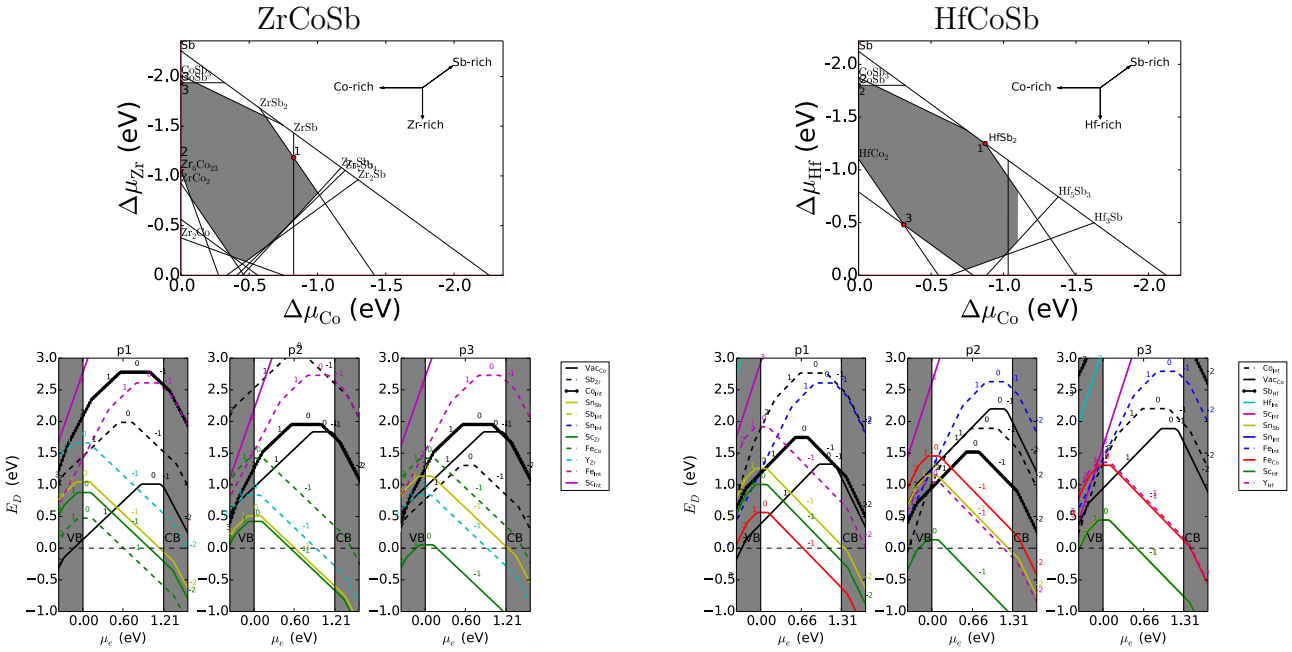

FIG. 3: The atomic chemical potential ($\Delta\mu_\alpha$, α is Zr/Hf, Co and Sb) stability window that would eliminate the formation of competing phases and result in thermodynamically stable ZrCoSb (left) and HfCoSb (right) are shown in grey (top). The energy of formation of most stable intrinsic defects (anti-sites, interstitials, vacancies) and extrinsic defects as a function of electronic chemical potential, μ_e. The energies are evaluated at three points in the boundaries of the $\Delta\mu_\alpha$ window.

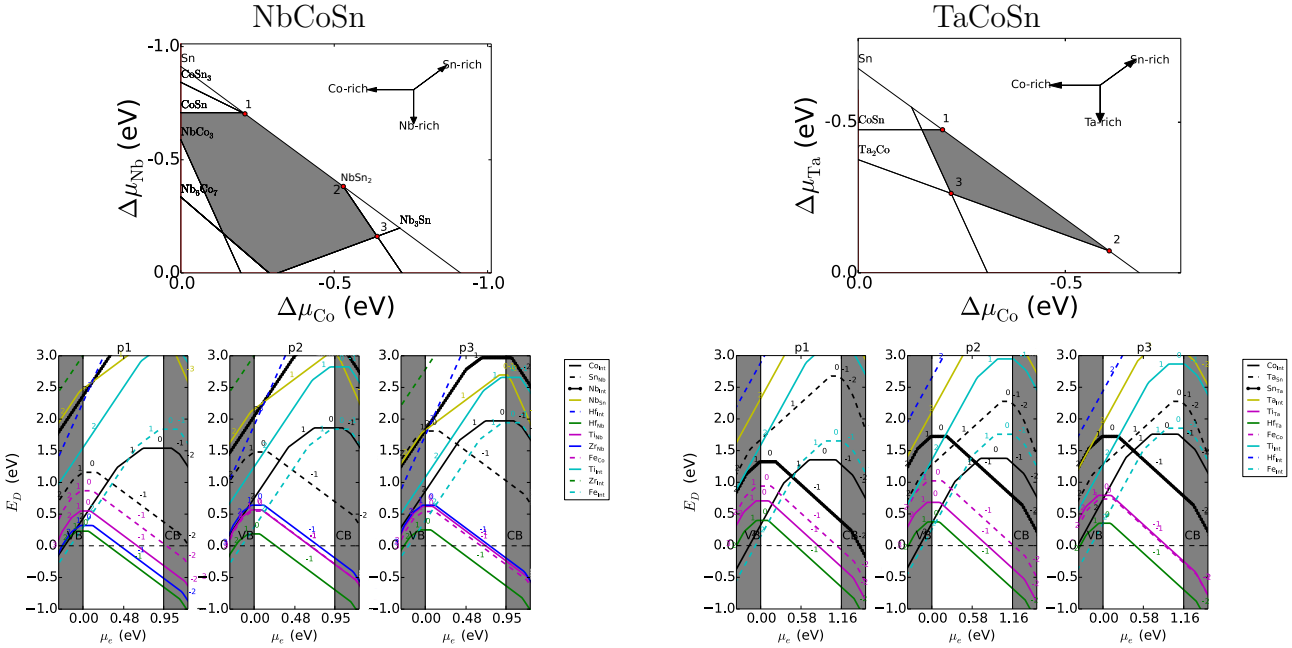

FIG. 4: The atomic chemical potential ($\Delta\mu_\alpha$, α is Nb/Ta, Co and Sn) stability window that would eliminate the formation of competing phases and result in thermodynamically stable NbCoSn (left) and TaCoSn (right) are shown in grey (top). The energy of formation of most stable intrinsic defects (anti-sites, interstitials, vacancies) and extrinsic defects as a function of electronic chemical potential, μ_e. The energies are evaluated at three points in the boundaries of the $\Delta\mu_\alpha$ window.

Thermodynamic stabilities

The internal energy, U, versus volume, V, curve for the HH and orthorhombic phases of NbCoSn, using LDA (left panel, top) and GGA (left panel, bottom) are shown in Fig. 5. Note that NbCoSn crystallizes in a HH phase and not in a orthorhombic Pnma phase. Consequently, we observe that for both functionals, U(HH)$-U$(orth)$>$ 300 meV/atom in this case.

U versus V curve evaluated using LDA functional for HH and orthorhombic (orth) phases of VCoGe (right panel, top) and TiCoAs (right panel, bottom) are shown in Fig.5. Note that LDA just like GGA, spuriously predicts the stability of the HH phase over the experimentally known orthorhombic phase for both compounds. Inset shows ΔH =$\mathrm{H_{HH}}$-$\mathrm{H_{orth}}$ versus pressure P, indicating that with the onset of a small amount of negative pressures, we have $\mathrm{H_{orth}} < H_{\mathrm{HH}}$.

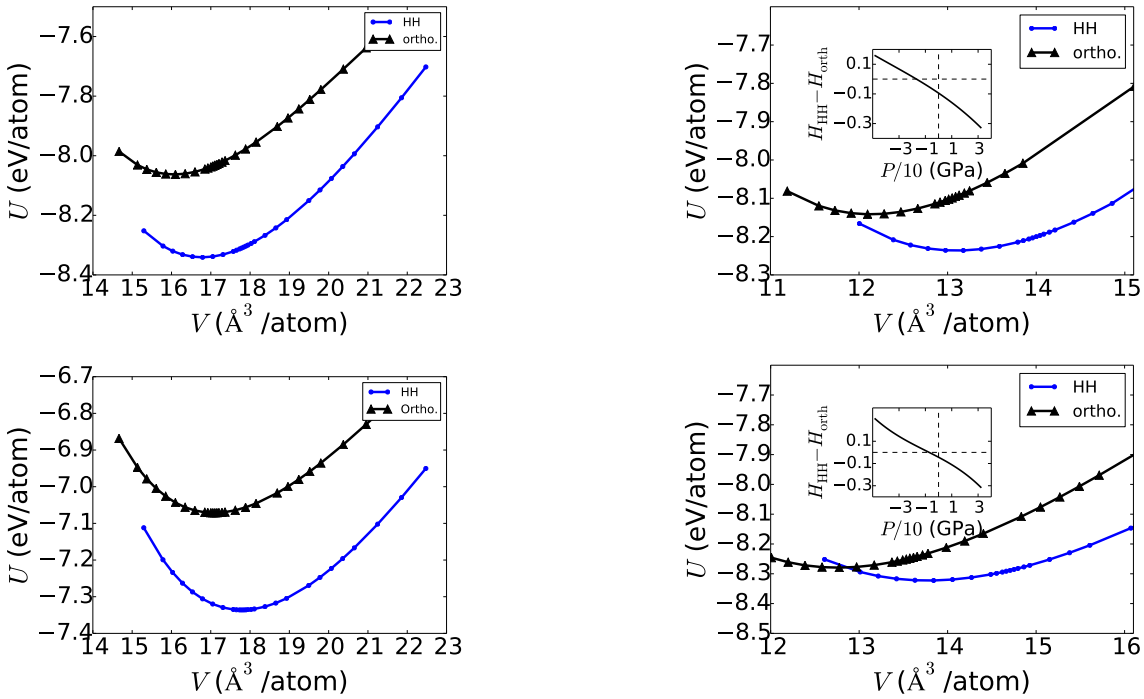

FIG. 5: U versus volume V curve for HH and orthorhombic phase for NbCoSn LDA (top) and GGA (bottom) in left panel. The right panel shows the same for VCoGe (top) TiCoAs (bottom). The insets in the right panel shows ΔH =$\mathrm{H_{HH}}$-$\mathrm{H_{orth}}$ versus pressure P.

[1] G. Makov and M. C. Payne, Physical Review B **51**, 4014 (1995).
[2] S. Baroni and R. Resta, Physical Review B **33**, 7017 (1986).
[3] C. Persson, Y.-J. Zhao, S. Lany, and A. Zunger, Phys. Rev. B **72**, 035211 (2005), URL http://link.aps.org/doi/10.1103/PhysRevB.72.035211.
[4] S. Lany and A. Zunger, Phys. Rev. B **78**, 235104 (2008), URL http://link.aps.org/doi/10.1103/PhysRevB.78.235104.
[5] G. Kresse and J. Furthmüller, Phys. Rev. B **54**, 11169 (1996).
[6] R. Stern, B. Dongre, and G. K. H. Madsen, Nanotechnology **27**, 334002 (2016).